A Low Power Walk for the NAO Robot

Jason Kulk and **James Welsh**
University of Newcastle, Australia
jason.kulk@studentmail.newcastle.edu.au

Abstract

Generally online walk pattern generators for humanoids are simplified, and don't produce ideal gaits. Allowing the robot to 'settle' into a more natural gait through the modification of the low-level positional controller would provide significant benefits. In this paper we attempt to achieve this, by limiting the power available to each motor in a humanoid, hence restricting how rigidly the joint can follow the generated walk pattern. This approach was evaluated by implementing the control modification on a humanoid robotics platform. The results show a significant improvement in walk speed, efficiency, and robustness. Moreover, the approach used here could be easily applied to any walk pattern generator, as the modification is in the low-level positional control.

1 Introduction

Humanoid robot locomotion is an exciting challenge that has been the centre of a significant body of research and development [Katić and Vukobratović, 2003; Chestnutt *et al.*, 2005; Behnke, 2006]. However, the mobility and poise of present humanoids does not compare to that of humans; the most prevalent limitations being speed, robustness, and efficiency. These deficiencies need to be overcome if humanoids are to be truly useful in a world designed for humans.

The industry-standard to generate and stabilise walking uses the Zero Moment Point (ZMP). The ZMP is defined as the point on the ground at which the net moment of the inertial and gravity forces has no component along the horizontal axes [Vukobratović and Borovac, 2004]. The notion of the ZMP can be combined with a stiff trajectory tracking method to implement a sufficiently stable walk [Pratt and Tedrake, 2006]. Firstly, a walk pattern that predicts the ZMP remains strictly inside the support polygon is generated, and then using a trajectory tracking algorithm which both implements the

pattern, and maintains the ZMP inside the support polygon, a stable walk can be produced.

Humans do not use high-gain trajectory tracking. For example, the tendon stiffness in the ankle is very low [Loram *et al.*, 2005], and while standing, the hip has a similar passive stiffness in the anteroposterior and mediolateral directions [Rietdyk *et al.*, 1999; Matjacic, 2001]. Perhaps, humanoid robots should have similarly low stiffness in the control of each joint.

There are several attempts to emulate low stiffness, typically involving modifications of the high-level controller. For example, using an impedance controller [Lim *et al.*, 2001], or using a variable compliance controller [Kawaji *et al.*, 1997; Nishikawa *et al.*, 1999; Sakaino and Ohnishi, 2006]. These controllers are then implemented with stiff low-level position controllers. However, placing the low stiffness in the low-level controller avoids modelling and sensing errors that occur in attempting to implement a compliant controller with hard position tracking.

Alternative trajectory tracking techniques may also be used [Nakanishi *et al.*, 2007], and adding compliance to the hardware in the legs can also have the desired effect [Van Der Linde, 1998].

The work presented here implements low stiffness in the low-level positional control, and was motivated by research on an anthropomorphic stance. In particular, the discovery that the ankle tendon stiffness is insufficient to maintain stance [Loram *et al.*, 2005]. This implementation provides an effective means for improving the speed, efficiency, and robustness of existing ZMP-based walk patterns.

The remainder of this paper will, firstly, introduce the robotics platform used for this work, including an explanation of how the stiffness can be changed. The improved speed, efficiency, and robustness will be demonstrated through the comparison of a low-stiffness walk with two full-stiffness walks; the original walk supplied with the robot, and a slightly improved version. Section 3 will outline the experiments used to compare the walks,

Section 4 will present the results of the comparison, and the final sections discuss and draw conclusions from the results obtained.

2 The NAO and ALWalk

The NAO is a humanoid robot developed by the French company Alderbaran Robotics, shown in Figure 1. The NAO weighs 4.5kg, stands 57cm high and has 21 degrees of freedom (DOF). There are five DOF in each leg; two in the ankle, two in the hip and one at the knee. An additional degree of freedom exists at the hip for yaw, however it is shared between both legs; that is both legs are rotated outward or inward, together, using this joint. The NAO uses brushed DC motors with magnetic rotary encoders for position feedback.

Figure 1: The NAO developed by Alderbaran Robotics, now used as the two-legged standard platform for RoboCup.

The NAO is provided with an open-loop walk engine. Walk patterns are generated online from a simple ZMP trajectory that is calculated from user specified step parameters. The ZMP trajectory is transformed into a centre of gravity (CoG) trajectory using an inverted pendulum model. This CoG trajectory is then tracked and maintained throughout single and double support phases using inverse kinematics [Gouaillier et al., 2008]. The swing leg trajectory is a cycloid.

The low-level controller for the joint position used by the NAO is of the form shown in Figure 2. The parameter K_s is a scaling factor (0 to 100%) that is applied to the PWM duty cycle calculated by the controller for the motor. This effectively modulates the power available to each motor. The parameter K_s is used in this paper

to provide a form of stiffness control; setting K_s to be small restricts the torque of motor, and under load, this will result in softer trajectory tracking. The desired joint positions come from the ALWalk engine.
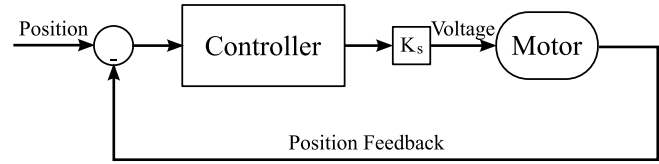
Figure 2: A block diagram of the low-level positional control used by the NAO.

3 Experimental Method

3.1 Walk Details

As an initial step, using an early version of the Alderbaran walk as a base, a slow walk was developed through the manual adjustment of walk parameters and global stiffness, that is, specifying a lowered stiffness value that is applied to every motor. The low-stiffness walk presented in this paper was then created through iterative improvements resulting from both varying the walk parameters, and setting the stiffness individually for each motor in the legs and arms. The effect of changing the walk parameters and stiffness values were not independent, for example, the ZMP offset walk parameters and ankle roll stiffness were strongly related. The reader is referred to [Gouaillier et al., 2008] for a complete description of walk parameters available.

Precedence was given to maintaining a low stiffness value in a joint. For example, consider the ankle pitch joint which had the lowest stiffness value in the legs ($K_s = 0.25$). This low value meant that the robot would fall if it leant too far forward, consequently walk parameters were selected to maintain an upright stance while walking. Similar compromises were made for other joints in the legs.

This process resulted in a considerable range of stiffness values, from 0.1 in the shoulders to 0.7 in the hip pitch joint. In the legs, the hip roll, ankle roll, and knee joints had stiffness values of 0.3, and the hip yaw joint had a stiffness of 0.6.

The two other walks presented here for comparison have a stiffness value of 1.0 in every leg joint, but have exactly the same arm settings as the low-stiffness walk. The first is the walk supplied by Alderbaran with the NAO, only small modification of the ZMP offsets and backlash compensation values were made so that the NAO walked stably on our practice field.

The second walk was made to serve two purposes. Firstly, it is a representative example of other walks

present at the recent RoboCup 2008, given every other walk had full-stiffness. Secondly, it demonstrates the effect of only changing the walk parameters. This second walk will henceforth be called the 'fast full-stiffness' walk, given that it was tuned for speed in the same manner as the low-stiffness walk.

3.2 Measurement of Walking Speed

The speed of each walk was measured over the same section of our practice field using an initially fully charged battery. The robot's walk was manually timed between two lines on the field 400cm apart, with the robot starting 20cm behind the first line, and walking well past the second line; so that the robot was walking at full speed over the entire distance. This procedure was repeated seven times.

3.3 Measurement of Energy Consumption

The NAO has current sensors in each of the motors, as well as one measuring the current drain from the battery. All of the currents were recorded at 50Hz while the robot walked for approximately 5m with a fully charged battery. The electric current data was collected three times for each of the three walks.

4 Results

4.1 Walking Speed

The speed of the improved low-stiffness walk was measured to be 13.9±0.2 cm/s. The speeds of the full-stiffness walks were 8.7±0.1 cm/s for the original walk, and 11.3±0.2 cm/s for the 'fast full-stiffness' walk. This means that the low-stiffness walk was 60% faster than the Aldebaran walk, and 23% faster than the improved full-stiffness walk.

This increase in speed proved to be advantageous at RoboCup 2008. The low-stiffness walk was significantly faster than the other walks present, whose speeds ranged between that of the Alderbaran walk and the 'fast full-stiffness' walk. This significant speed advantage was a major factor in our victory in the two-legged standard platform league at RoboCup 2008.

A video comparing the low-stiffness walk and Alderbaran walk can be found at [Kulk, 2008a]. The video not only shows the improvement in speed, but also illustrates differences in the hip height, sway, and motion smoothness.

4.2 Walking Efficiency

Overall Efficiency
The battery current drain for each walk is shown in Figure 3. Recall, that the low-stiffness walk is significantly faster than the two full-stiffness walks. Thus, it covers the same distance in much less time, while drawing significantly less current the entire time. Figure 4 provides

a better illustration of the improved efficiency, showing the power used by the motors per centimetre travelled; essentially removing the 0.87A drain of other components from Figure 3 and scaling the result to reflect the improved speed of the low-stiffness walk.

A useful measure of efficiency is the unit-less specific mechanical cost of transport c_{mt} [Collins *et al.*, 2005], given by

$$c_{mt} = \frac{\text{energy used (J)}}{\text{weight (N)} \cdot \text{distance travelled (m)}}.$$

The low-stiffness walk has $c_{mt} = 2.4$, the Alderbaran walk $c_{mt} = 5.8$ and the 'fast full-stiffness' $c_{mt} = 4.8$. Consequently, the low-stiffness walk represents a 59% and 50% improvement, respectively, in efficiency compared to the other walks.

A practical result of this improvement in efficiency is the distance the robot can now walk on a single battery charge. The full-stiffness walks allow the robot to travel 415m and 520m respectively, while the low-stiffness walk enables the robot to cover 815m, nearly twice the original distance.

Individual Joint Efficiencies
The current in each of the motors in the left leg is shown in Figure 5. This data is used to determine which joints are most responsible for the improvement in efficiency, where the efficiency is the specific mechanical cost of transport described above. The largest contributor was the knee joint improving the overall efficiency by 12.2% and 11.9% compared with the Alderbaran and 'fast full-stiffness' walk. This improvement is due to the reduction in K_s, and also the reduced knee flexion that was made possible through the improved stability of the low-stiffness walk. The small improvement in efficiency between the Alderbaran and 'fast full-stiffness' walk stems from the improvement in speed.

The ankle pitch joint showed the next largest improvement with gains in efficiency of 6.1% and 6.6%. This joint had the lowest stiffness in the leg, hence the result is not unexpected. However, the next greatest improvement of 5%, was found in the hip pitch joint, which had the highest stiffness of any joint in the robot. The hip pitch joint moves the furthest of the joints in the leg during the walking cycle, so the significant improvement here comes from a smaller reduction in K_s.

The hip roll joint also showed an improvement of 3.0% and 1.4%, however, the ankle roll provided only a small improvement over the Alderbaran walk and no improvement over the 'fast full-stiffness' walk.

4.3 Walk Stability and Robustness

A heuristic measure of stability was used in this instance. The NAO is equipped with foot pressure sensors, but,

The battery current drain while walking over the same distance
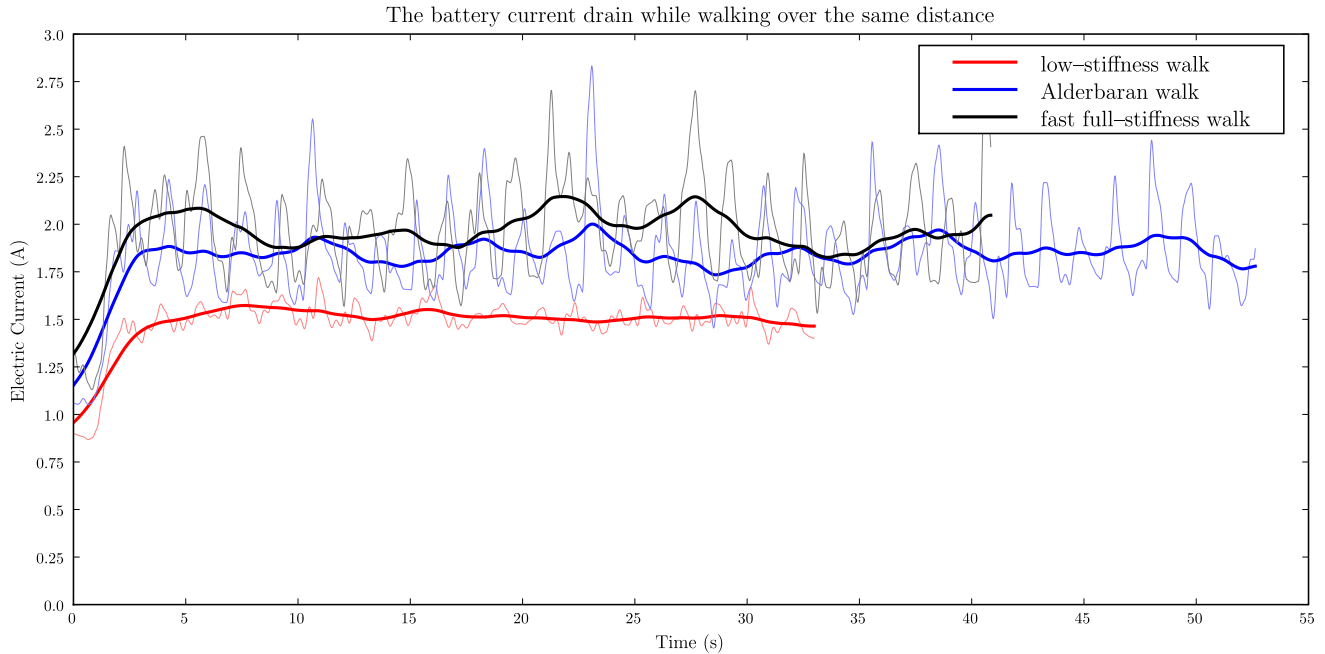
Figure 3: The current drain from the battery while walking 4.6m. The thin lines represent the unfiltered current values, and the thick lines have been filtered with a running 2s-window mean. Note that the plots for the two stiff walks are longer because they take more time to cover the 4.6m, and the current drain of the microprocessors in the NAO is 0.87A.

they provide very little useful information about the centre of pressure. The ZMP could be calculated using the position feedback, however, speed was the primary design concern, so it was acceptable to say — as long as the robot walked stably enough not to fall over it was acceptable. It was usually clear after a few steps on the practice field whether the walk was sufficiently stable.

In that vein the stability of the walks will be compared. Both the Alderbaran walk and the low-stiffness walk never fell over during the collection of data for this paper. This means the robot walked for approximately 100m without falling over. However, the 'fast full-stiffness' walk was not stable requiring assistance about 30% of the time to prevent it from falling over, this was considered acceptable because this particular walk was only constructed for comparative purposes.

The major improvement between the Alderbaran walk and low-stiffness walk was the robustness to external disturbances. During testing the low-stiffness walk was robust enough to walk over its own network and power cables, walk into goals, desks, and walls without falling over in most situations.

To further demonstrate and quantify this observation, a short length of uneven surface was constructed, and both walks attempted to traverse it. The surface had irregularities of amplitude up to to 1 cm. A short

video of the experiment was made, and can be found at [Kulk, 2008b]. The low-stiffness walk successfully walked over the irregular surface four out of five times, while the Alderbaran walk only completed the course once in its five trials.

5 Discussions

The manufacturer's recommended battery current drain is 1.5A. Figure 3 shows that the only walk that is within this recommendation is the low-stiffness walk, the full-stiffness walks are always drawing more than the recommended battery current.

Furthermore, Figure 3 also shows current peaks of over 2.6A for the two full-stiffness walks, which are larger than the maximum rated current of the battery. In fact, the robot shut itself down once during testing of the 'fast full-stiffness' walk to protect the battery.

Figure 5 also shows large current peaks for the two full-stiffness walks in each of the motors. This combined with the fact that the motors are now using much less power and running significantly cooler, improves motor longevity.

Having K_s for each joint as an additional parameter to vary also made tuning the walk easier. Using full stiffness, it is reasonably difficult to find a set of walk parameters that are stable. This was demonstrated at
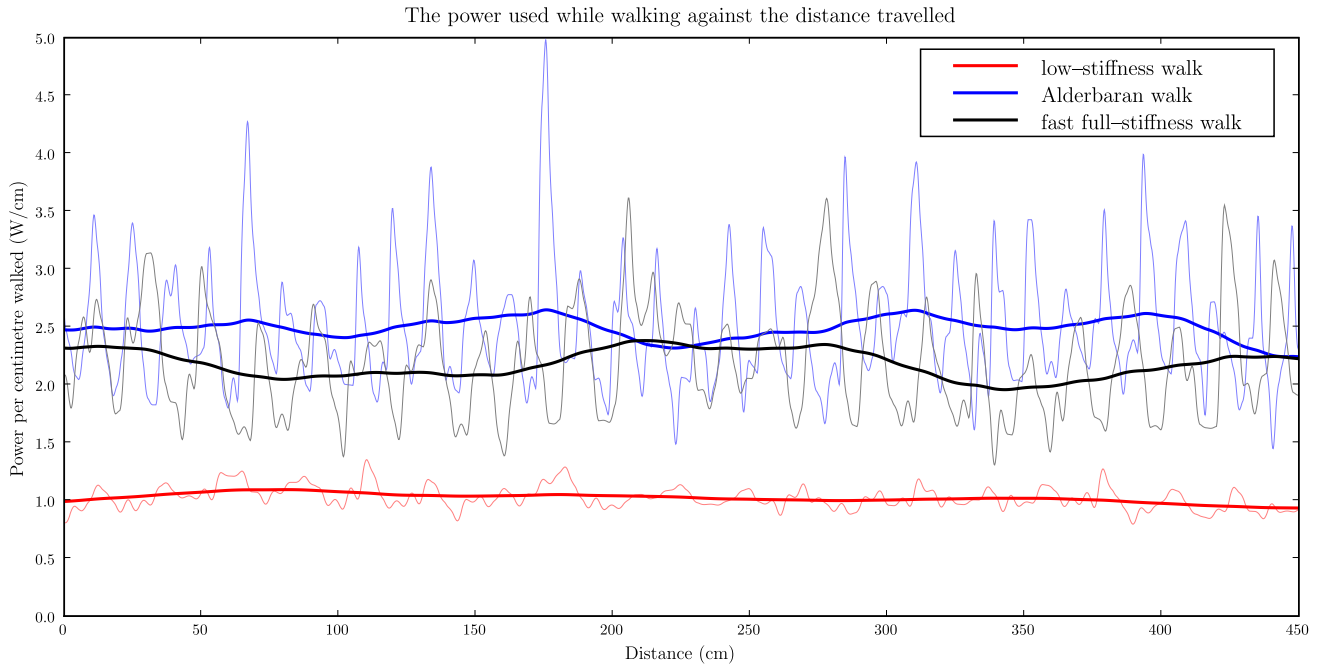
Figure 4: The power per metre used by the robot while walking. The thin lines are the unfiltered values, and the thick lines are the running 2s-window means. The low-stiffness walk is 59% more efficient than the original walk supplied by Alderbaran, and 50% more efficient than the improved full-stiffness walk.

RoboCup 2008, where many walks were actually worse than the Alderbaran walk.

One explanation as to why the low-stiffness walk is more efficient, is that the low motor powers prevent the robot from rigidly tracking imperfect trajectories produced by the online walk pattern generators. Instead it exploits the natural dynamics of the system, allowing the robot to 'settle' into a more efficient gait, rather than insisting that the calculated trajectory is the better one.

The smoothness of the motion contributes to the improved stability and robustness of the walk. Consider the hip pitch joint during the swing phase. With stiff tracking the leg is abruptly accelerated forward at the beginning of the swing, the moment exerted on the rest of the body can be great enough to induce slip in the supporting foot, rotating the entire robot. This can potentially result in the swing leg hitting the ground, or the robot becoming unbalanced and falling sideways. As the amount of slip is unpredictable this can present a problem. A similar effect was noticed at the end of the swing phase. Reducing the power in the hip pitch joint smoothed out these accelerations, and consequently improved the stability of the walk.

The robustness of the walk was also improved by the compliance introduced by the low powers in the ankle. When the foot comes into contact with the ground the low power allows the foot to conform to the irregularities in the floor, without effecting the orientation of the rest of the leg. If the robot is not falling over, the leg will be approximately vertical. Thus, when the foot becomes the single support, the support leg will remain approximately vertical, held in place by the controller and the friction in the joint itself. In contrast, stiff tracking would actively rotate the leg, through the ankle, on contact so that it is perpendicular to the ground. This will result in the robot falling over if the ground is not perpendicular to the gravity vector.

6 Conclusions

A low-stiffness walk was created by manually tuning the power available to each motor in the robot, through a modification in the low-level controller. This low-stiffness walk was compared to two full-stiffness walks using a humanoid robotic platform.

When the low-stiffness walk was compared to the original full-stiffness walk it was observed that the speed could be improved by 60%, while at the same time improving the specific cost of transport by 59%, and increasing the robustness of the walk to external influences.

Decreasing the power in each motor reduces the stiffness at which the walk pattern trajectory is tracked. This prevents the robot perfectly tracking a non-ideal gait, instead allowing it to settle into a more natural and efficient gait.
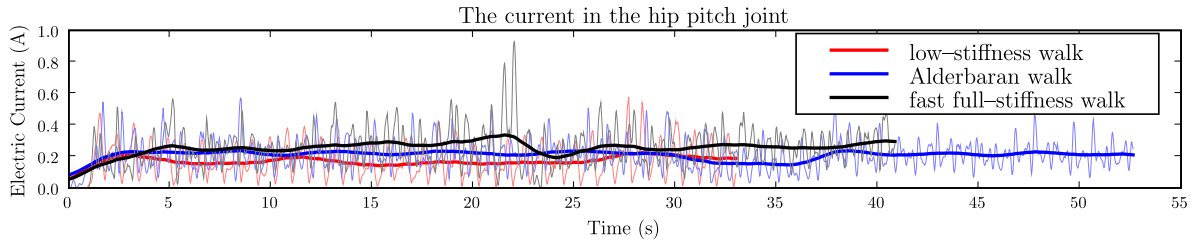
(a) In the hip pitch joint the low-stiffness walk was 4.6% and 5.6% more efficient than the original and 'fast' stiff walks respectively.
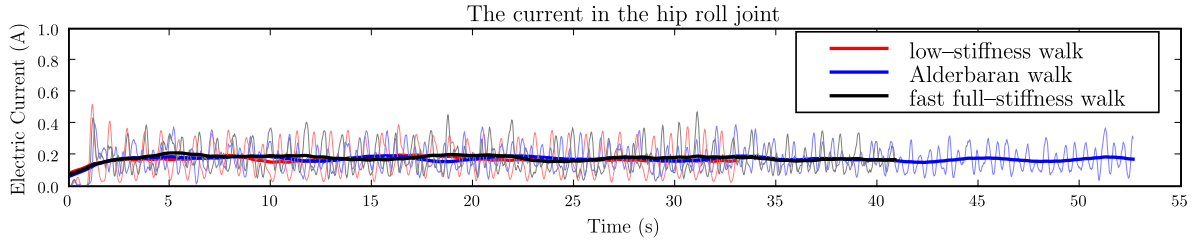
(b) In the hip roll joint the low-stiffness walk was 3.0% and 1.4% more efficient than the original and 'fast' stiff walks respectively.
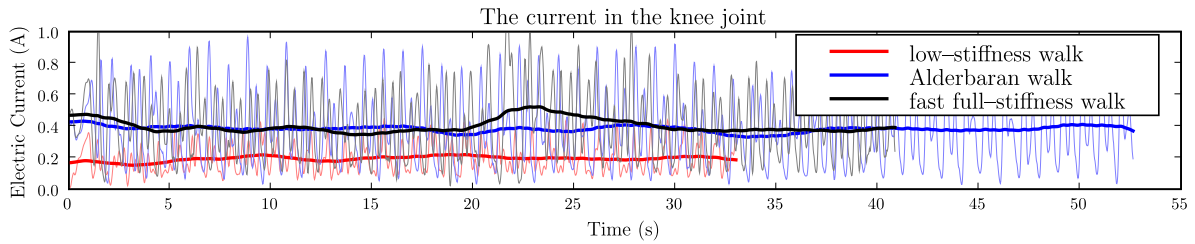
(c) In the hip pitch joint the low-stiffness walk was 12.2% and 11.9% more efficient than the original and 'fast' stiff walks respectively. The greatest improvement in efficiency came from this joint.
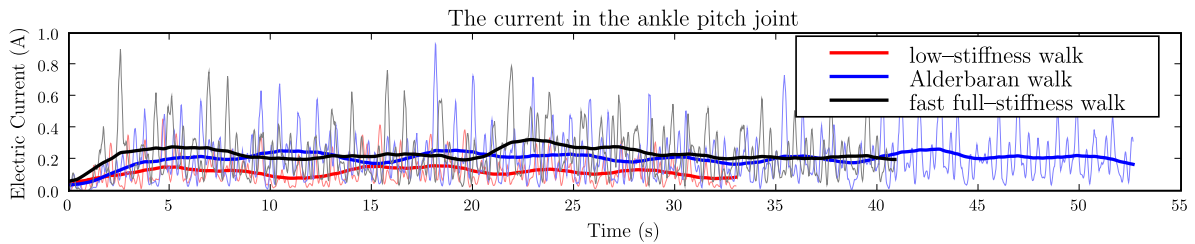
(d) In the ankle pitch joint 6.1% and 6.6% less energy was used in the low-stiffness walk compared to the Aldebaran and 'fast' stiff walks respectively.
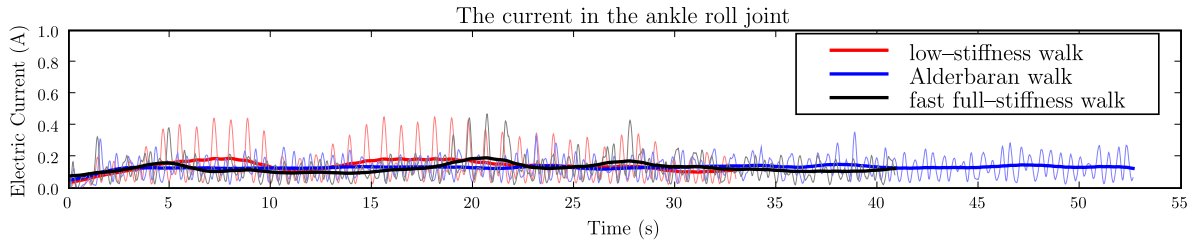
(e) In the ankle roll joint 1.8% less energy was used in the low-stiffness walk compared to the Aldebaran. However, the low-stiffness walk and 'fast' stiff walk used the same amount of energy.

Figure 5: The current in each joint in the left leg while the robot walked a distance of 4.6m. The longer times for the two full-stiffness walks arise because those walks a slower.

The reduction in power also makes the walk more robust to external influences, because the low-stiffness in the position tracking stops the joint from exerting too great a torque against an obstacle.

7   Future Work

An area that will be explored further is changing K_s in each joint as a function of walk phase. This increase in complexity will necessitate the use of a machine learning algorithm to optimise the speed of the walk. Real-time speed feedback will be provided by a laser scanner tracking the robot, and electric current feedback will be provided by the sensors on the robot itself.

References

[Behnke, 2006] Sven Behnke. Online trajectory generation for omnidirectional biped walking. In *Proceedings of IEEE International Conference on Robotics and Automation*, pages 1597–1603, Orlando, Florida, 2006.

[Chestnutt *et al.*, 2005] Joel Chestnutt, Manfred Lau, German Cheung, James Kuffner, Jessica Hodgins, and Takeo Kanade. Footstep planning for the honda asimo humanoid. In *Proceedings of IEEE International Conference on Robotics and Automation*, pages 629–624, Barcelona, Spain, 2005.

[Collins *et al.*, 2005] Steve Collins, Andy Ruina, Russ Tedrake, and Martijn Wisse. Efficient bipedal robots based on passive-dynamic walkers. *Science*, 307(5712):1082–1085, 2005.

[Gouaillier *et al.*, 2008] David Gouaillier, Vincent Hugel, Pierre Blazevic, Chris Kilner, Jerome Monceaux, Pascal Lafourcade, Brice Marnier, Julien Serre, and Bruno Maisonnier. The nao humanoid: a combination of performance and affordability. *submitted to IEEE Transactions on Robotics*, 2008.

[Katić and Vukobratović, 2003] Duško Katić and Miomir Vukobratović. Survey of intelligent control techniques for humanoid robots. *Journal of Intelligent and Robotics Systems*, 37(2):117–141, 2003.

[Kawaji *et al.*, 1997] S. Kawaji, K. Ogasawara, J. Iimori, and S. Yamada. Compliance control for biped locomotion robot. In *Proceedings of IEEE International Conference on Systems, Man, and Cybernetics*, volume 4, pages 3801–3806, Oct 1997.

[Kulk, 2008a] Jason Kulk. Nao walk comparison [video]. Available at http://www.youtube.com/watch?v=x9mCOxKE4I0, August 2008.

[Kulk, 2008b] Jason Kulk. A nao walking over an uneven surface [video]. Available at http://www.youtube.com/watch?v=3Plt2DzMr-M, August 2008.

[Lim *et al.*, 2001] Hun-ok Lim, S.A. Setiawan, and A. Takanishi. Balance and impedance control for biped humanoid robot locomotion. In *Proceedings of IEEE International Conference on Intelligent Robots and Systems*, volume 1, pages 494–499, 2001.

[Loram *et al.*, 2005] Ian D Loram, Constantinos N Maganaris, and Martin Lakie. Human postural sway results from frequent, ballistic bias impulses by soleus and gastrocnemius. *J Physiol*, 564(1):295–311, 2005.

[Matjacic, 2001] Zlatko Matjacic. Control of ankle and hip joint stiffness for arm-free standing in paraplegia. *Neuromodulation*, 4(1):37–46, 2001.

[Nakanishi *et al.*, 2007] J. Nakanishi, M. Mistry, J. Peters, and S. Schaal. Towards compliant humanoids-an experimental assessment of suitable task space position/orientation controllers. In *Proceedings of IEEE International Conference on Intelligent Robots and Systems*, pages 2520–2527, 29 2007-Nov. 2 2007.

[Nishikawa *et al.*, 1999] N. Nishikawa, Y. Fujimoto, T. Murakami, and K. Ohnishi. Variable compliance control for 3 dimensional biped robot considering environmental fluctuations. *Transactions of the Institute of Electrical Engineers of Japan*, 119(12):1507–1514, 1999.

[Pratt and Tedrake, 2006] J. E. Pratt and R. Tedrake. Velocity-based stability margins for fast bipedal walking. *Fast Motions in Biomechanics and Robotics*, pages 299–324, 2006.

[Rietdyk *et al.*, 1999] S. Rietdyk, A. E. Patla, D. A. Winter, M. G. Ishac, and C. E. Little. Balance recovery from medio-lateral perturbations of the upper body during standing. *Journal of Biomechanics*, 32(11):1149–1158, 1999.

[Sakaino and Ohnishi, 2006] S. Sakaino and K. Ohnishi. Sliding mode control based on position control for contact motion applied to hopping robot. In *Proceedings of IEEE International Conference on Industrial Technology*, pages 170–175, Dec. 2006.

[Van Der Linde, 1998] R.Q. Van Der Linde. Active leg compliance for passive walking. In *Proceedings of IEEE International Conference on Robotics and Automation*, volume 3, pages 2339–2344, May 1998.

[Vukobratović and Borovac, 2004] Miomir Vukobratović and Branislav Borovac. Zero moment point – thirty five years of its life. *International Journal of Humanoid Robotics*, 1(1):157–173, 2004.